

# 2.44 kV Ga<sub>2</sub>O<sub>3</sub> vertical trench Schottky barrier diodes with very low reverse leakage current

Wenshen Li<sup>1</sup>, Zongyang Hu<sup>1</sup>, Kazuki Nomoto<sup>1</sup>, Riena Jinno<sup>2</sup>, Zexuan Zhang<sup>1</sup>, Thieu Quang Tu<sup>3</sup>, Kohei Sasaki<sup>3</sup>, Akito Kuramata<sup>3</sup>, Debdeep Jena<sup>1,4,5</sup> and Huili Grace Xing<sup>1,4,5</sup>

<sup>1</sup>School of Electrical and Computer Engineering, Cornell University, Ithaca, NY 14853, USA, email: [w1552@cornell.edu](mailto:w1552@cornell.edu)

<sup>2</sup>Department of Electronic Science and Engineering, Kyoto University, Kyoto 615-8510, Japan

<sup>3</sup>Novel Crystal Technology, Inc. Sayama, Saitama 350-1328, Japan

<sup>4</sup>Department of Material Science and Engineering, Cornell University, Ithaca, NY 14853, USA

<sup>5</sup>Kavli Institute at Cornell for Nanoscale Science, Cornell University, Ithaca, NY 14853, USA

**Abstract**—High performance  $\beta$ -Ga<sub>2</sub>O<sub>3</sub> vertical trench Schottky barrier diodes (SBDs) are demonstrated on bulk Ga<sub>2</sub>O<sub>3</sub> substrates with a halide vapor phase epitaxial layer. A breakdown voltage (BV) of 2.44 kV, Baliga's figure-of-merit (BV<sup>2</sup>/R<sub>on</sub>) of 0.39 GW/cm<sup>2</sup> from DC measurements and 0.45 GW/cm<sup>2</sup> from pulsed measurements are achieved, all of which are the highest among  $\beta$ -Ga<sub>2</sub>O<sub>3</sub>-based power devices. A lowest reverse leakage current density below 1  $\mu$ A/cm<sup>2</sup> until breakdown is observed on devices with a fin width of 1-2  $\mu$ m, thanks to the reduced surface field (RESURF) effect provided by the trench SBD structure. The specific on-resistance is found to reduce with increasing area ratio of the fin-channels following a simple relationship. The reverse leakage current agrees well with simulated results considering the barrier tunneling and barrier height lowering effects. The breakdown of the devices is identified to happen at the trench bottom corner, where a maximum electric field over 5 MV/cm could be sustained. This work marks a significant step toward reaching the high figure-of-merit  $\beta$ -Ga<sub>2</sub>O<sub>3</sub> promises.

## I. INTRODUCTION

$\beta$ -Ga<sub>2</sub>O<sub>3</sub> has seen increasing research effort in recent years towards the realization of high performance electronic devices. A Baliga's figure of merit (FOM) of  $\beta$ -Ga<sub>2</sub>O<sub>3</sub> well exceeds that of GaN and 4H-SiC arises from a combination of ultra-wide bandgap of  $\sim$ 4.5 eV, therefore high expected critical electric field of up to 8 MV/cm [1] and decent room temperature electron mobility of  $\sim$ 200 cm<sup>2</sup>/V-s [2, 3], making  $\beta$ -Ga<sub>2</sub>O<sub>3</sub> an excellent material candidate for next generation power electronic devices, especially under harsh environment. The availability of melt-growth methods for single-crystal bulk substrate provides added advantage towards lower cost and a head start for fast development of epitaxial growth and device technologies. With the availability of high quality halide vapor phase epitaxial (HVPE) layers with a net doping concentration around  $\sim$ 2 $\times$ 10<sup>16</sup> cm<sup>-3</sup> in recently,  $\beta$ -Ga<sub>2</sub>O<sub>3</sub> power electronic devices has well-surpassed the unipolar material limit of Si, exemplified by the demonstration of kilovolt-class enhancement-mode transistors [4] and Schottky barrier diodes (SBDs) [5, 6]. However, the FOM of the present devices are still far from the projected material limit. In this work, we

demonstrate record high performance vertical  $\beta$ -Ga<sub>2</sub>O<sub>3</sub> SBDs through (i) effectively reduced leakage current with the reduced surface field (RESURF) effect offered by a trench SBD structure [7] and (ii) smoothly-etched trench profile. A record high breakdown voltage (BV) of 2444 V, and record high FOM (BV<sup>2</sup>/R<sub>on</sub>) are achieved without other dedicated field management techniques. The diodes show near ideal behavior in both forward and reverse operations well predicted by physics-based models.

## II. DEVICE DESIGN AND FABRICATION

**Fig. 1** shows the schematic cross-section the Ga<sub>2</sub>O<sub>3</sub> trench SBDs. The drift layer consists a 10- $\mu$ m HVPE n-Ga<sub>2</sub>O<sub>3</sub> grown on a (001) n-type Ga<sub>2</sub>O<sub>3</sub> substrate. Fin widths ( $W_{fin}$ ) of 1-4  $\mu$ m and a trench depth of 1.55  $\mu$ m are designed. The fin area ratio is defined to be the fin width over the pitch size.

**Fig. 2** illustrates the fabrication process of the trench SBDs. First, the trench was dry etched using a BCl<sub>3</sub>/Ar gas mixture and Ti/Pt as the hard mask. After the dry etch and mask removal, wet acid treatment was performed in HCl and HF each for 20 min to remove the dry etch induced damage. A rounded trench corner profile is realized as a results of the dry and wet etching as shown in the scanning electron microscope (SEM) cross-section image (**Fig. 4**), which is desired for reduced field crowding. The back ohmic contact was formed by first dry etching the backside for 5 min, followed by a Ti/Au deposition and rapid thermal anneal for 1 min under N<sub>2</sub>. Then, a 100-nm Al<sub>2</sub>O<sub>3</sub> dielectric was deposited by atomic layer deposition (ALD) and opened by dry etching for the Schottky contact on top of the fins. Finally, Ni Schottky contact was deposited by e-beam evaporation, followed by Ti/Pt sputtering for the sidewall metal coverage. **Fig. 3** shows the optical top view of a fabricated device with a fin length of 150  $\mu$ m and  $W_{fin}$  of 2  $\mu$ m.

## III. RESULTS AND DISCUSSION

Capacitance-voltage measurements were performed on the regular SBDs co-fabricated on the same sample. **Fig. 5** plots the extracted net doping concentration profile from the measurements on both the SBDs made on the original epitaxial surface as well as the SBDs made on the etched planar surface formed by the trench-etch step. The doping concentration increases from  $\sim$ 1 $\times$ 10<sup>16</sup> cm<sup>-3</sup> close to the surface to  $\sim$ 2 $\times$ 10<sup>16</sup> cm<sup>-3</sup> beyond

a depth of  $\sim 2.5$   $\mu\text{m}$ . The  $1/C^2$  plot is shown in **Fig. 6**. A built-in potential ( $V_{bi}$ ) of  $1.25 \pm 0.1$  V is extracted, corresponding to a Schottky barrier height ( $q\phi_B$ ) of  $1.4 \pm 0.1$  eV.

**Fig. 7** shows the forward I-V characteristics of the trench SBDs in comparison with regular SBDs measured with DC scans. The 2-4  $\mu\text{m}$  trench SBDs shown in the figure all have an area ratio of 50%, while the 1- $\mu\text{m}$  device of 33%. *All current density for the trench SBDs in this work is normalized to the entire anode area.* The trench SBDs and regular SBDs have a similar turn-on voltage of 1.25 V. From a fitting to the thermionic emission model,  $q\phi_B$  is extracted to be 1.35 eV, which agrees with the extraction from C-V measurements. The  $R_{on}$  of the 2-4  $\mu\text{m}$  fin devices are similar, being around  $11.3$   $\text{m}\Omega\cdot\text{cm}^2$  and higher than that of the regular SBDs ( $7$   $\text{m}\Omega\cdot\text{cm}^2$ ).

**Fig. 8** shows the pulsed I-V measurements of the forward characteristics. In comparison with the DC measurements, the slightly lower turn-on voltage measured by the pulsed measurements is believed to be related to the trapping effect which is more severe during the DC scan, while the higher current at  $>3$  V is due to the mitigation of device self-heating effect with pulsed measurements. We believe the pulsed I-V measurements provide a more accurate measurement of the on resistance determined by the intrinsic drift layer properties.

As shown in **Fig. 9**, the  $R_{on}$  values extracted by pulsed measurements are compared among the different devices. It is found that the SBD made on the etched surface with a  $8.55$   $\mu\text{m}$  drift layer has the lowest  $R_{on}$  of  $4$   $\text{m}\Omega\cdot\text{cm}^2$ , while the SBD with a  $10$   $\mu\text{m}$  drift layer has an  $R_{on}$  of  $7$   $\text{m}\Omega\cdot\text{cm}^2$ . The difference is due to the top  $1.55$   $\mu\text{m}$  drift layer, which has a net doping concentration of  $\sim 1 \times 10^{16}$   $\text{cm}^{-3}$ . The trench SBDs have an  $R_{on}$  of  $10$   $\text{m}\Omega\cdot\text{cm}^2$ , which matches well with the expected value considering the 50% area ratio leads to a doubled contribution of the specific  $R_{on}$  from the  $1.55$   $\mu\text{m}$  top layer. A simple model for the specific  $R_{on}$  of the trench SBDs is developed:

$$R_{on,sp} = 4 + \frac{3}{\text{area ratio}} \text{ m}\Omega \cdot \text{cm}^2 \quad (1)$$

**Fig. 10** shows the statistics of the extracted  $R_{on}$  for the trench SBDs with different  $W_{fin}$  and area ratio. The  $R_{on}$  of the 2-4  $\mu\text{m}$  devices follows the trend expressed by (1) very well. For the 1- $\mu\text{m}$  devices, (1) has to be modified reflecting a reduced effective fin width for best fitting, which indicates that there may be some etching damage and/or trapping effect at the fin sidewall, which is most dominant for the 1- $\mu\text{m}$  fin devices.

**Fig. 11** plots the simulated electric field profile along vertical cut-lines at the fin center (dash line in Fig. 1). The field near the surface is effectively reduced by the trench structure. The RESURF effect is more prominent for smaller fin width.

**Fig. 12** shows the representative reverse I-V characteristics of the trench SBDs in comparison with the regular SBDs. The reverse leakage current for the trench SBDs is much lower than the regular SBDs, and the BV is much higher, reaching a record value of  $2.44$  kV with the 1- $\mu\text{m}$  device. The reverse leakage current is lower than  $1$   $\text{mA}/\text{cm}^2$  before breakdown for the 1-3

$\mu\text{m}$  devices, a typical value used to specify the reverse blocking voltage for commercial SBDs. Even lower leakage current beyond the detection limit is observed for some of the devices, as shown in **Fig. 13**. The leakage current for the lower leakage devices follows the simulated reverse I-V characteristics considering the barrier tunneling and barrier-height lowering effect. An electron effective mass of  $0.3m_0$  [3] and the extracted barrier height of  $1.4$  eV is used in the simulation.

The statistics of the BV is shown in **Fig. 15**. The BV is found to increase with smaller fin width. No correlation between the BV and the area ratio has been observed. To identify the breakdown mechanism, the electric field profile is simulated. **Fig. 14** and **Fig. 16** shows the simulated electric field profile along a horizontal cutline across the trench bottom corner, at a fixed voltage of  $2$  kV and around the highest breakdown voltage, respectively. It is observed that the field crowding happens around the trench corner and the field peak increases with fin width at a fixed voltage. As shown in **Fig. 16**, the field peaks all reach a similar value of  $\sim 5.9$  MV/cm at the highest BV for each fin width, indicating that the breakdown happens at the trench corner. Note that the  $5.9$  MV/cm value is simulated considering a  $90^\circ$  trench corner angle. In reality the value should be lower due to the rounded trench corner profile.

#### IV. CONCLUSION

Exploiting the pronounced RESURF effect in the trench SBD structure and the smoothly etched trench corner profile, the reverse leakage current is effectively suppressed in the  $\text{Ga}_2\text{O}_3$  trench SBDs and high breakdown voltages are achieved. **Fig. 17** benchmarks the state-of-the-art  $\beta\text{-Ga}_2\text{O}_3$  SBDs [5-9]. Our 1- $\mu\text{m}$  device achieved a record high BV and our best 2- $\mu\text{m}$  device with a 50% area ratio achieved a record FOM of  $0.39$   $\text{GW}/\text{cm}^2$  ( $2096$  V,  $11.3$   $\text{m}\Omega\cdot\text{cm}^2$ ) from DC scan and  $0.45$   $\text{GW}/\text{cm}^2$  ( $2096$  V,  $9.8$   $\text{m}\Omega\cdot\text{cm}^2$ ) from pulsed measurement. The lowest projected  $R_{on}$  from pulsed measurements is  $7$   $\text{m}\Omega\cdot\text{cm}^2$ , achievable by increasing the area ratio close to 100%. The improved BV and FOM from the current state-of-the-art further unveils the excellent material properties of  $\beta\text{-Ga}_2\text{O}_3$ , which provides an attractive platform for power electronic devices.

#### ACKNOWLEDGMENT

Supported in part by NSF DMREF 1534303 and AFOSR (FA9550-17-1-0048), carried out at CNF sponsored by the NSF NNCI program (ECCS-1542081), and CCMR Shared Facilities supported through the NSF MRSEC program (DMR-1719875).

#### REFERENCES

- [1] M. Higashiwaki, Appl. Phys. Lett., vol. 100, no. 1, p. 013514, 2012.
- [2] N. Ma, Appl. Phys. Lett., vol. 109, no. 21, p. 212101, 2016.
- [3] Y. Zhang, Appl. Phys. Lett., vol. 112, no. 17, p. 173502, 2018.
- [4] Z. Hu, IEEE EDL, vol. 39, no. 6, pp. 869-872, 2018.
- [5] K. Konishi, Appl. Phys. Lett., vol. 110, no. 10, p. 103506, 2017.
- [6] J. Yang, Appl. Phys. Lett., vol. 110, no. 19, p. 192101, 2017.
- [7] K. Sasaki, IEEE EDL, vol. 38, no. 6, pp. 783-785, 2017.
- [8] J. Yang, IEEE EDL, vol. 38, no. 7, pp. 906-909, 2017.
- [9] Z. Hu, IEEE JEDS, vol. 6, pp. 815-820, 2018.

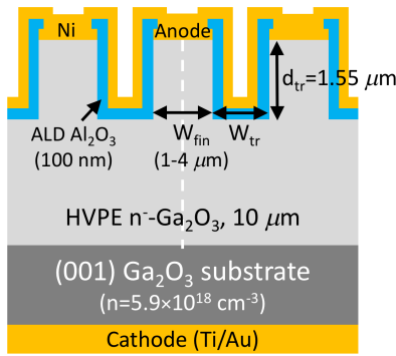


Fig. 1. Schematic cross-section of the Ga<sub>2</sub>O<sub>3</sub> trench Schottky barrier diodes. Fin widths ( $W_{fin}$ ) of 1–4  $\mu\text{m}$  are designed with different fin area ratio ( $W_{fin}/(W_{fin}+W_{tr})$ ). A trench depth ( $d_{tr}$ ) of 1.55  $\mu\text{m}$  is designed.

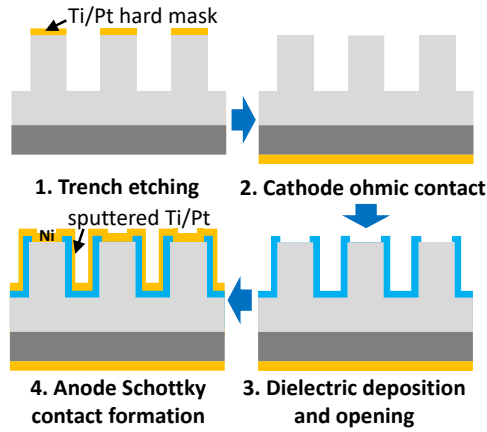


Fig. 2. Fabrication process flow of the trench SBDs.



Fig. 3. Optical top view of a fabricated device with a  $W_{fin}$  of 2  $\mu\text{m}$  and a fin area ratio of 50%. The length of the fins is 150  $\mu\text{m}$ .

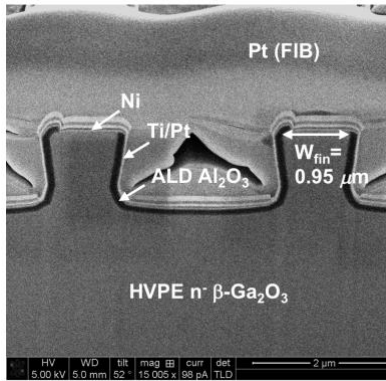


Fig. 4. Scanning electron microscopy (SEM) cross-section image of a device with a designed fin width of 1  $\mu\text{m}$ . A slightly inward-slanted sidewall profile and rounded trench corners are observed, preferable for improved RESURF effect and reduced field crowding.

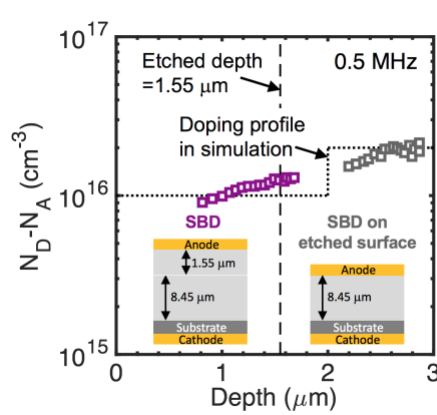


Fig. 5. Extracted net doping concentration ( $N_D - N_A$ ) from C-V measurements. Two types of regular Schottky barrier diodes are used for the measurements with the cross-section shown in the insets. Dotted line shows the approximated doping profile used in the TCAD simulation.

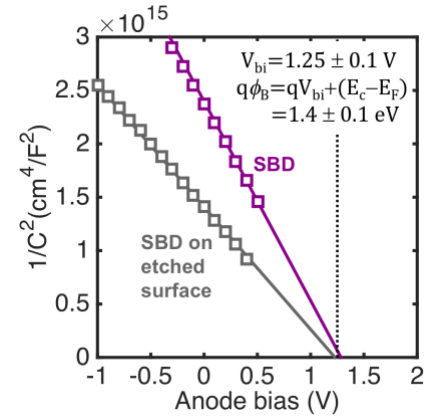


Fig. 6.  $1/C^2$  plot for the SBDs and the SBDs on the etched surface. The  $V_{bi}$  is extracted to be  $\sim 1.25$  V, corresponding to a barrier height ( $q\phi_B$ ) of  $\sim 1.4$  eV.

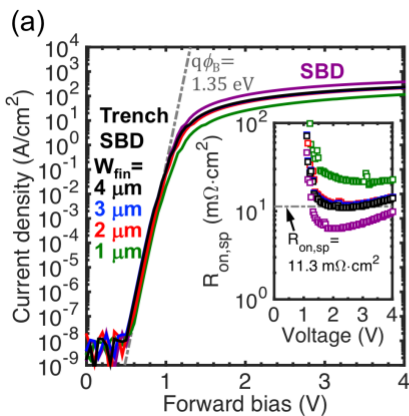


Fig. 7. Forward I-V characteristics (a) in log scale and (b) in linear scale of the trench SBDs in comparison with regular SBDs, measured by DC scans. The current of the trench SBDs are normalized by the anode area. A barrier height ( $q\phi_B$ ) of 1.35 eV is extracted from the thermionic emission model using a reduced effective Richardson constant  $A^{**}$  of 33.1  $\text{A}/\text{cm}^2\text{-K}^2$  [17\_APL\_NICT], which agrees with the extracted barrier height by C-V.

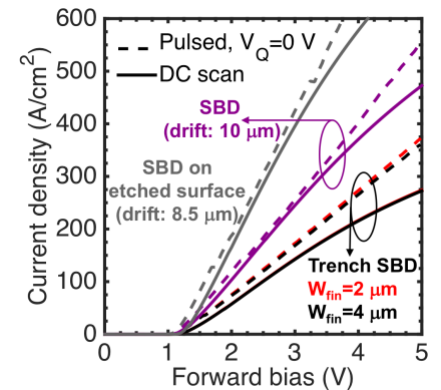
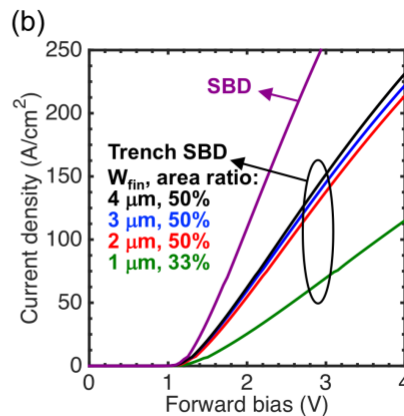


Fig. 8. Comparison of the forward I-V characteristics measured by pulsed measurements with DC scan. A pulse width of 8.4  $\mu\text{s}$  and duty cycle of 0.84% is used. The dispersion is likely due to a combination of device self-heating and trapping effect.

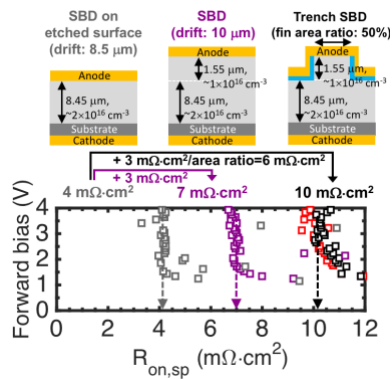


Fig. 9. Extracted specific differential on-resistance ( $R_{on,sp}$ ) of the devices from pulsed I-V measurements. The  $R_{on,sp}$  of the trench SBDs is well-explained by considering the 50% fin area ratio.

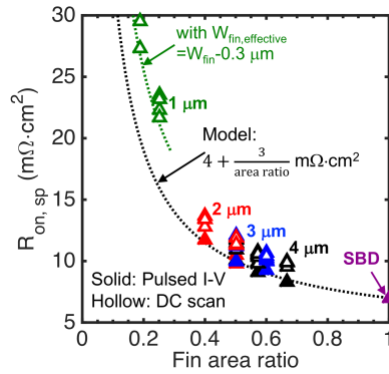


Fig. 10. Statistics of the extracted specific  $R_{on}$  of the trench SBDs. The trend of  $R_{on}$  agrees well with a simple model considering the area ratio for the devices with 2-4  $\mu\text{m}$  fin widths, while a modified model with reduced effective  $W_{fin}$  is found to match the 1- $\mu\text{m}$  device data.

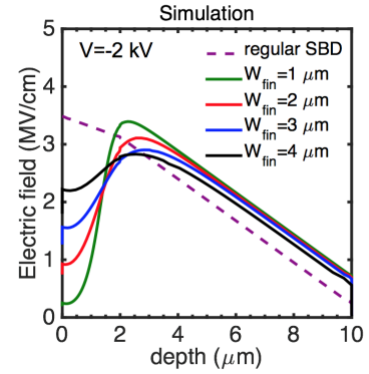


Fig. 11. Simulated electric field profile along vertical cut-lines at the fin center (see the dash line in Fig. 1) at a reverse bias of 2 kV. The surface field is reduced effectively with the trench structure.

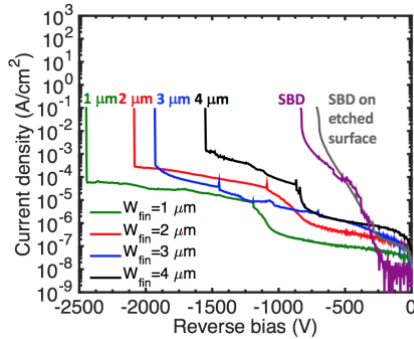


Fig. 12. Representative reverse I-V characteristics of the trench SBDs in comparison with the regular SBDs. Much lower leakage current below 1 mA/cm<sup>2</sup> is observed for the 1-3  $\mu\text{m}$  devices in comparison with regular SBDs, together with much higher breakdown voltages.

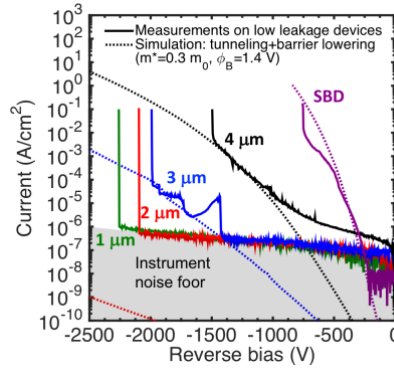


Fig. 13. Representative I-V characteristics of the trench SBDs with low leakage current. The leakage current profile agrees well with the simulation considering barrier tunneling and barrier height lowering. Effective mass of 0.3  $m_0$  and the extracted  $q\phi_B$  of 1.4 eV is used in the TCAD simulation.

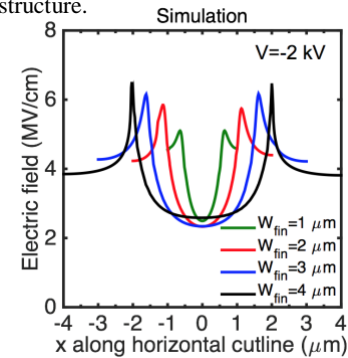


Fig. 14. Simulated electric field profile along a horizontal cutline across the trench bottom corner at 2 kV. The electric field at the trench corner is found to increase with the fin width.

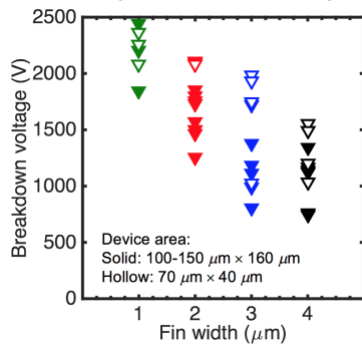


Fig. 15. Statistics of the measured breakdown voltage of the trench SBDs. The BV is found to increase with reduced fin width.

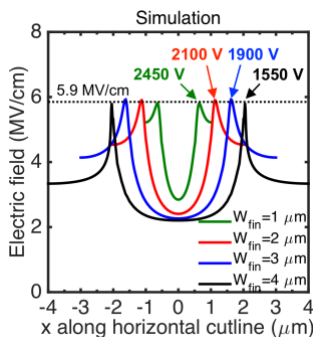


Fig. 16. Simulated electric field profile along a horizontal cutline across the trench bottom around the highest BV of each fin width. The field peak are close to be the same for all fin width, indicating that the breakdown is limited by the breakdown at the trench corner.

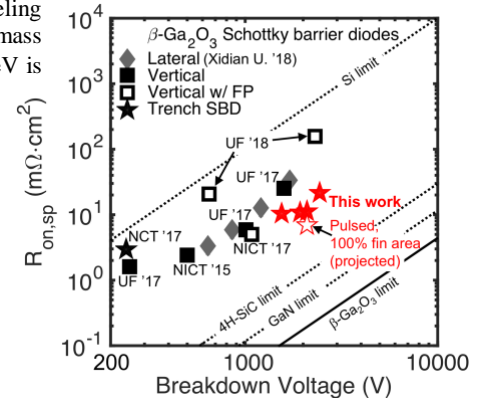


Fig. 17. Benchmark plot of  $\beta\text{-Ga}_2\text{O}_3$  Schottky barrier diodes [5-9]. Our 1- $\mu\text{m}$  trench SBD achieves the highest BV, while the 2- $\mu\text{m}$  trench SBD achieves the highest FOM.  $R_{on}$  extracted from pulsed measurements projected to 100% fin area is also shown, indicating the potential of the trench SBDs even without dedicated field management techniques.